



Docking and Molecular Dynamics Calculations of Some Previously Studied and Newly Designed Ligands to Catalytic Core Domain of HIV-1 Integrase and an Investigation to Effects of Conformational Changes of Protein on Docking Results

Selami Ercan^{1*}

¹Batman University, School of Health Sciences, 72060, Batman, Turkey

Abstract: Nowadays, AIDS still remains as a worldwide pandemic and continues to cause many deaths which arise from HIV-1 virus. For nearly 35 years, drugs that target various steps of virus life cycle have been developed. HIV-1 integrase constitutes one of these steps which is essential for virus life cycle. Computer-aided drug design is being used in many drug development and drug improvement studies as also used in development of the first HIV-1 integrase inhibitor Raltegravir. In this study, 3 ligands which are already used as HIV-1 integrase inhibitors and 4 newly designed ligands were docked to catalytic core domain of HIV-1 integrase. Each ligand docked to three different conformations of protein. Prepared complexes (21 items) were carried out by 50 ns MD simulations and results were analyzed. Finally, the binding free energies of ligands were calculated. It was determined that designed ligands L01 and L03 gave favorable results. The questions about the ligands which have low docking scores in a conformation of protein could give better scores in another conformation of protein and if the MD simulations carry the different oriented and different localized ligands in same position at the end of simulation were answered.

Keywords: HIV-1 integrase; drug design; docking; molecular dynamics; binding free energy.

Submitted: September 09, 2016. **Revised:** October 13, 2016. **Accepted:** October 24, 2016.

Cite this: Ercan S. Docking and Molecular Dynamics Calculations of Some Previously Studied and Newly Designed Ligands to Catalytic Core Domain of HIV-1 Integrase and an Investigation to Effects of Conformational Changes of Protein on Docking Results. JOTCSA. 2017;4(1):243–70.

DOI: To be assigned.

*Corresponding author. E-mail: slmrcn@gmail.com. Tel: +90 488 217 3767, fax: +90 488 217 3601.

INTRODUCTION

Human immunodeficiency virus (HIV) is a member of lentiviruses genus from retroviruses family, which causes a worldwide pandemic of acquired immunodeficiency syndrome (AIDS). It was recently reported that there are about 35 million (33.2 million-34.0 million) people living with human immunodeficiency virus type 1 (HIV-1) at 2015, 1.5 million (1.4 million-1.7 million) deaths that related to AIDS, and 2.1 million (1.9 million – 2.4 million) newly infected people [1].

HIV-1 pol gen encodes three essential enzymes, namely reverse transcriptase (RT), integrase (IN), and protease (PR) which are essential for virus life cycle [2]. Because of the roles of these enzymes they attract most attention in HIV-1 drug discovery studies. Although the first FDA-approved HIV-1 drug Zidovudine [3, 4] (AZT), was a nucleoside reverse-transcriptase inhibitor (NRTI) in the following years another drugs of different targets were discovered. Besides NRTIs, nucleotide reverse-transcriptase inhibitors (NtRTIs), non-nucleoside reverse-transcriptase inhibitors (NNRTIs) are discovered which also target RT enzyme. Other anti-HIV drug groups are as follows: Protease inhibitors (PIs), fusion inhibitors (FIs), co-receptor inhibitors (CRIs) and integrase inhibitors (INIs) [5, 6]. However, instead of using single drugs, a combination of RT and PR drugs, named Highly Active Antiretroviral Therapy (HAART) is used to suppress viral replication of HIV-1 [7-9]. HAART has an achievement on reducing disease progression, but it is also related to collateral problems like resistance of antivirals, toxicity and dosing which are preventing successful treatment of HIV [8, 10-19]. These shortfalls of HAART drugs' combinations point out the need for new drugs. Therefore, in this study, we tried to get some new inhibitors whose analogues showed good docking scores and interactions with IN in our previous work [20]. In contrast to many approved drugs which target RT and PR, only three IN inhibitors are currently approved as antiviral drugs. After approving Raltegravir (RAL: N-[2-[4-[(4-fluorophenyl)methylcarbonyl]-5-hydroxy-1-methyl-6-oxopyrimidin-2-yl]propan-2-yl]-5-methyl-1,3,4-oxadiazole-2-carboxamide) [21, 22] as the first IN inhibitor in 2007, US Food and Drug Administration (FDA) also approved Elvitegravir (EVG: 6-[(3-chloro-2-fluorophenyl)methyl]-1-[(2S)-1-hydroxy-3-methylbutan-2-yl]-7-methoxy-4-oxoquinoline-3-carboxylic acid) [23], and Dolutegravir (DLG: (4R,12aS)-N-[(2,4-difluorophenyl)methyl]-7-hydroxy-4-methyl-6,8-dioxo-3,4,12,12a-tetrahydro-2H-pyrido [5,6]pyrazino[2,6-b][1,3]oxazine-9-carboxamide) [24] for market distribution.

HIV-1 integrase is a 32 kDa protein consisting of 288 amino acids and is a polynucleotidyl transferase enzyme. IN have structurally and functionally three different domains; N-terminal domain (NTD, 1-49 residues) containing Zn atom and a "His₂Cys₂" (HHCC) motif

which is highly conserved among all integrases, catalytic core domain (CCD, 50-212 residues) containing one or two divalent metal ion such as Mg^{2+} or Mn^{2+} and Asp64, Asp116 and Glu152 which is called "D,D-35-E" motif that is essential for catalysis, C-Terminal domain (CTD) is nonspecific DNA binding domain and consist of 213-288 residues.

Integrase mediates the insertion of viral DNA to host chromosomal DNA. It cuts a copy of double-stranded DNA of reverse transcribed viral RNA from the 3' ends and inserts into the host DNA. Integration occurs in two distinct steps. In the first step called 3' processing integrase cuts two or three nucleotides from the long terminal repeats (LTR) of vDNA at highly conserved CA bases which expose 3'-hydroxyl groups. Second step, involving insertion of processed vDNA to host DNA, is strand transfer reaction. IN catalyzes 3'-hydroxyl groups exposed from first step to attack host DNA from phosphate groups [25]. Thus, these reactions also make IN a specific target because human body does not need such a process.

Due to solubility and inter-domain flexibility problems, full-length structure of integrase could not be solved yet. This issue also is one reason of later development of IN inhibitors. However, individual structure of domains and combination of core domain with N-terminal domain [26] and C-terminal domain [27] have been solved by crystallography and nuclear magnetic resonance (NMR) techniques. Among these structures, only 1BL3 [28] and 2ITG [29] contain the flexible loop that consists of residues between 140-149. After identifying a crystal structure of catalytic core domain with a ligand (5CITEP: 1-(5-chloro-1H-indol-3-yl)-3-hydroxy-3-(2H-tetrazol-5-yl)) [30], IN catches attention as a new target of antiviral drug studies. An advantage of targeting IN is that there is not any homologue enzyme of IN in human body. However, beside use of different sets of chemical molecule types for inhibition of integrase, only β -diketo acids and their bioisosteres are the approved inhibitors and some of them are in clinical trial [31]. Furthermore, in recent years the crystal structures of prototype foamy virus integrase (PFV IN) with viral DNA and also contain the integrase inhibitors RAL, EVG, and DLG have been reported [32, 33]. Notwithstanding the only 15% sequence similarity between HIV integrase and PFV integrase the structure of integrase with vDNA provide new perspectives for researchers to understand inhibitor interactions with receptor and also DNA and researchers used these structures as templates for modelling full-length HIV-1 integrase by computational tools [32-34].

Drug development and improvement are expensive and time-consuming processes. Computational methods such as docking, molecular dynamics, and free energy computations are widely used to help development of new drugs, understanding interactions of drugs with receptors and also reaction mechanisms taking place in

inhibition. It is known that receptors are flexible *in vivo* and even though some docking programs allow flexible protein and ligand docking, but it is a time-consuming process and such a process also could be performed by molecular dynamics after docking process. Therefore, this study also aspires to detail interactions of ligands with receptor in different conformations of protein and to define whether a docking program could mislead a researcher for obtaining best ligand. Namely, in general, a researcher uses docking program for one conformation of protein to dock a series of ligands, but this is only a snapshot of dynamic protein. A ligand could be an inappropriate candidate in a conformation of protein according to docking score and could be a good candidate in another conformation of protein. Also we want to define if the molecular dynamics studies carry these complexes; which different conformations of receptor have differently oriented ligands in it, to same point at (in terms of conformation of ligand and also ligand-receptor interactions) the end of simulation. Two such like studies have been performed by Brigo and co-workers [35, 36]. They have studied differences between wild and mutant type proteins containing 5CITEP as ligand without docking. The coordinates of studied structures are taken from cluster analyses' trajectories in one of these works [35]. In the second work [36], they studied MD behaviors of protein which some diketo acid derivatives and also 5CITEP docked in.

In this study, approved HIV-1 IN inhibitors (INSTs) RAL, EVG and DLG and four newly designed ligands (Figure 1) which are derivatives of previously studied [20] ones used for docking, molecular dynamics and Molecular Mechanic Poisson-Boltzmann Surface Area (MM/PBSA) [37]. Approved inhibitors were selected to make an accurate comparison about interactions of ligands with receptor. Furthermore, the fact that these molecules studied by many researchers and the existence of crystal structures of these molecules with protein (PFV IN) may allow us to look from a more accurate perspective to analyze results. The docking modes of ligands with different conformations of receptor, dynamic behaviors of protein and complexes, and binding energies of ligands analyzed widely in this work. Moreover, the restrained electrostatic potential (RESP) charges of used ligands derived from quantum mechanics studies for more compatible results with *in vivo*.

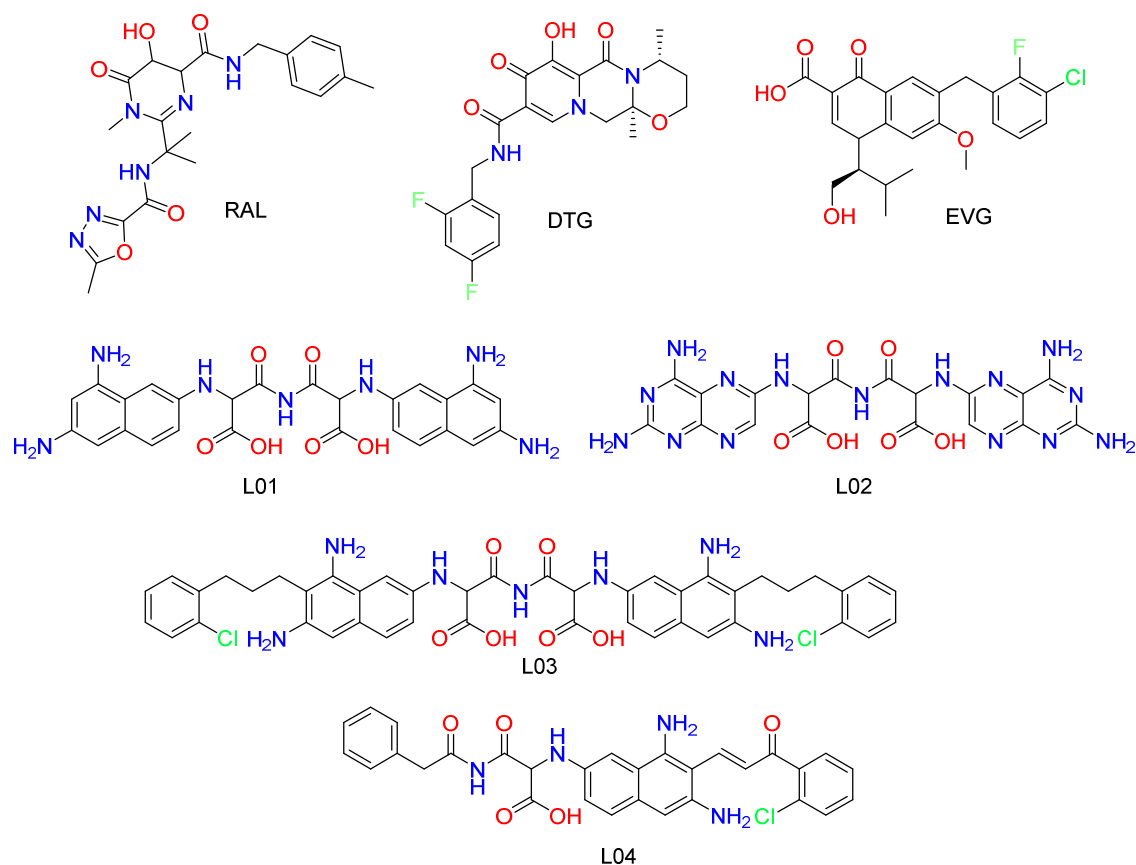


Figure 1. HIV-1 Integrase inhibitors and newly designed ligands those used in the study.

MATERIALS AND METHODS

Preparation of Used Protein Model

The crystallographic structure of CCD was obtained from the Protein Data Bank (www.rcsb.org) [38] with the code 1BL3.pdb. This structure contains A, B, and C chains. We used chain C because it has 50-209 residues (others have missing residues) and one Mg atom in the catalytic site. It is known that integrase catalyzes strand transfer reaction when we have two metal atoms [39]. Therefore, second Mg atom was inserted to model by superimposing C chain of 1BL3.pdb with chain A of the recently solved crystal structure of PFV integrase with pdb code 4BE2 [40]. Superimposition showed that the E152 residue of 1BL3.pdb is in an inappropriate conformation which results in being far from second Mg atom. So it also replaced with E152 residue of 4BE2.pdb. All crystal water molecules were kept in simulation.

The model loaded to *Xleap* module of AMBER 12 [41] and hydrogen atoms were added automatically by module. Model was neutralized by adding Cl⁻ ions and solvated with TIP3P [42] water model in a truncated octahedral box having at least 10 Å distance around the

receptor and a distance of 0.4 Å between protein and solute. The Amber ff99SB force field was used for the protein.

Preparation of the ligands

The ligands were designed on the basis of structures those are previously studied such as folic acid, methotrexate, and designed compounds LGA and LGB[20]. Ligand optimizations were performed by Gaussian 09 [43] program in three steps. In the first step, all ligands were optimized with semi-empirical AM1 method, followed by B3LYP/6-31+(d,p) optimization and finally latest optimizations were carried out by HF/6-31G* level to produce partial charges of ligands with RESP. *Antechamber* and *parmchk* modules of AMBER package program was used to prepare ligands for *Xleap* program and to create additional force field files which contain missing parameters of any ligands. After docking studies, the RESP charges (Supp. Inf.) of each ligand were added in *Xleap* program by editing molecules.

Molecular Dynamics Studies of Receptor

The minimization of receptor carried out in three steps. In the first step, all the system without water was kept fixed to minimize water molecules. In the second step, water and H atoms of protein are taken free while protein and Mg atoms were kept fixed. In the first and second step, a force constant of 5.0 kcal mole⁻¹ Å⁻² was used to restrain fixed atoms. In final minimization, all the system was released free. Minimizations carried out as 1000 steps steepest descent method followed by 1000 steps conjugate gradient method.

Minimization and MD simulations were carried out with *pmemd* module of AMBER 12. Minimized structure was used as starting point of MD simulation. Before production simulations, the system was heated to 300 K for 500 ps where protein except hydrogens and Mg atoms restrained with 1.0 kcal mole⁻¹ Å⁻² force constant. Heating followed by a 500 ps equilibration simulation.

MD simulations were performed at 300 K temperature. Langevin thermostat with a collision frequency of 2 was used to maintain the temperature of system. The long-range electrostatic interactions were treated by the Particle Mesh Ewald (PME) protocol [44] with a 10 Å cut-off distance. To constrain bond lengths involving hydrogens, SHAKE [45] algorithm was applied. A time step of 2 fs and periodic boundary conditions were employed throughout simulation.

After 20 ns MD simulation of receptor cluster analyses were carried out by *kclust* tool of MMTSB Toolset [46] based on RMSD mode. Three different cluster sets of receptor were defined and best models of each clusters were used for docking, MD simulations of complexes and MM/PB(GB)SA calculations.

Docking Studies

All docking studies were carried out with AutoDock 4 [47] docking program and with the aid of MGL Tools [47] in preparing structures for docking and analyses of results. Lamarckian Genetic Algorithm was used for docking with the settings of 150 individuals in a population, maximum energy evaluations of 2,500,000, maximum generations of 27,000 and 50 docking runs for each ligand. Autodock 4 scores docking of ligands by calculating their binding energies and the best scored conformations of ligands were selected for further studies.

Molecular Dynamics Studies of Complexes

Ligands having best scores for each conformation of receptor combined in Xleap program and also RESP charges of ligands were added. The way and conditions detailed in molecular dynamics studies of receptor followed for molecular dynamics studies of complexes for 50 ns.

MM/PB(GB)SA Studies

The binding free energies of ligands were calculated by MM/PBSA and MM/GBSA methods which implemented in AMBER 12 suite program as MMPBSA.py [37]. A schematic representation of thermodynamic cycle of method shown in Figure 2. With an interval of 10 ps, 1000 snapshots were extracted from MD production trajectories. The binding free energy was computed from the free energy difference of the free ligand, free receptor and ligand-receptor complex as formulated below:

$$\Delta G_{binding,solvated} = \Delta G_{complex,solvated} - (\Delta G_{receptor,solvated} + \Delta G_{ligand,solvated}) \quad (Eq. 1)$$

where $G_{complex}$, $G_{receptor}$, and G_{ligand} are the free energy of complex, receptor and ligand molecules, respectively. These energy values are calculated using an average over the extracted snapshots taken from single MD trajectories. Each state can be estimated from molecular mechanics energy E_{MM} , solvation free energy G_{sol} , and solute entropy S .

$$\Delta G_{binding} = \Delta H - T\Delta S \approx \Delta E_{MM} + \Delta G_{sol} - T\Delta S \quad (Eq. 2)$$

$$\Delta E_{MM} = \Delta E_{internal} + \Delta E_{electrostatic} + \Delta E_{vdw} \quad (Eq. 3)$$

$$\Delta G_{sol} = \Delta G_{PB/GB} + \Delta G_{SA} \quad (Eq. 4)$$

In Eq. (2), the terms ΔE_{MM} , ΔG_{sol} , and $-T\Delta S$ are dedicated to the changes of gas phase energy, solvation free energy, and the conformational entropy upon binding, respectively. ΔE_{MM} is the sum of internal energy, ΔE_{int} , (bond, angle, and dihedral energies), electrostatic, $\Delta E_{electrostatic}$, and van der Waals energies, ΔE_{vdw} which are computed from MD simulations. Solvation free energy, ΔG_{sol} , depends on polar and nonpolar contributions. $\Delta G_{PB/GB}$, is the electrostatic solvation free energy (polar contribution), and ΔG_{SA} is the nonelectrostatic solvation energy (nonpolar contribution). The polar contribution is calculated from either PB or GB model. Dielectric constants for solute and solvent were set to 1 and 80, respectively. The nonpolar solvation energy, ΔG_{SA} , was computed from the solvent accessible surface area (SASA) with a probe radius of 1.4 Å (Eq. (5)).

$$\Delta G_{SA} = \gamma SASA + \beta \quad (Eq. 5)$$

where γ is the surface tension constant and β is the offset constant. These values are set to 0.0072 kcal mol⁻¹ Å⁻² and 0 kcal mol⁻¹ for MMGBSA and 0.0378 kcal mol⁻¹ Å⁻² and -0.5692 kcal mol⁻¹ for MMPBSA. Besides free energy calculations, normal mode analyses (*nmode*) also were performed for defining entropy contribution to binding energies by using an interval of 100 ps 100 frames were extracted from MD trajectories. Less snapshots selected from snapshots used for free energy calculations due to time consuming of *nmode* analyses.

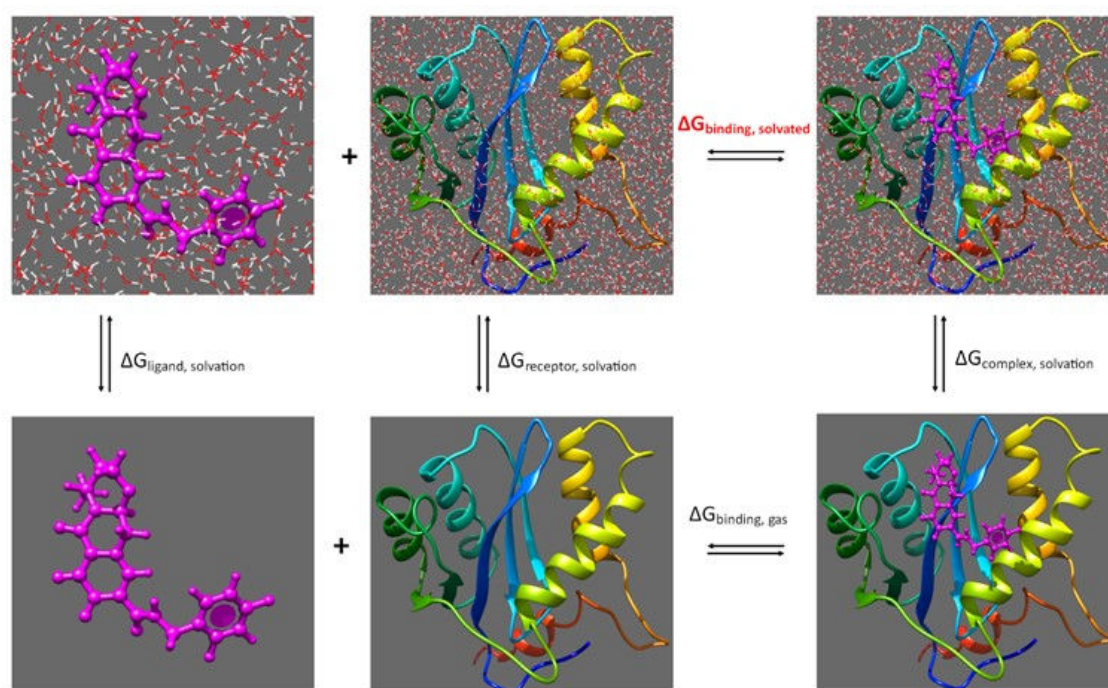


Figure 2. Thermodynamic cycle of MM-PB(GB)SA method.

RESULTS AND DISCUSSION

Molecular Dynamics Studies of Receptor

An important point in MD simulation is to evaluate the stability of system which can be defined by root mean square deviations (RMSD) of time-varying backbone atoms coordinates respect to MD starting frame (Figure 3.). Small changes in RMSD values suggest that there are not significant movements in the CCD and system reaches a plateau after 2.5 ns with a value of ~ 2.3 Å. This situation could be attributed to structure of CCD having less flexible subdomains, only 140-149, 166-171 and 186-194 residues are flexible in CCD. The RMSD plot of 138-150 which also contains the flexible loop shows that it undergoes a conformational change approximately at 4.5 ns which is ratified by MD simulation movie (Figure 3).

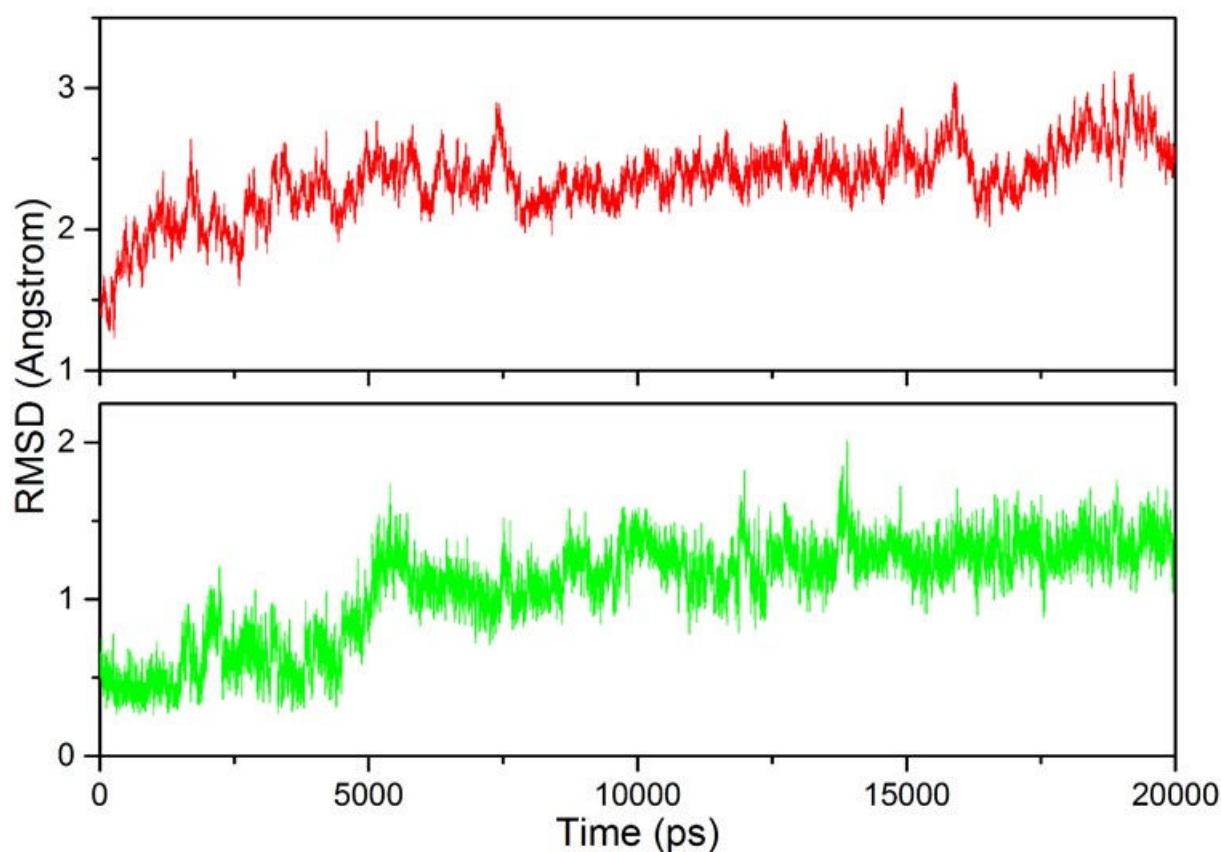


Figure 3. The time evolution of the RMSD values of backbone atoms for all residues (red) and for 140-149 residues (green) in the HIV-1 IN catalytic core.

The distances of Mg^{2+} ions with concerned residue atoms extracted from MD simulation revealed that the catalytic center is reached a stabilization point (Supp. Inf. Figures 1, 2.).

One of the Mg^{2+} ion coordinates with OD1 and OD2 oxygen atoms of D64 and D116 respectively, and oxygen of four water molecules, while second Mg^{2+} ion coordinates with OD2 atom of D64 and OE1 and OE2 atoms of E152 alongside three waters' oxygen atoms. After MD simulation of receptor three conformationally different structures of CCD were defined by cluster analyses. Superimposition of clusters' members named C1, C2 and C3 is represented as ribbon and basic style in Figure 4. C1 constitutes 23.77% of 10,000 frames, where C2 and C3 constitute 61.51 % and 14.72 % of 10,000 frames, respectively. As denoted from evaluation of RMSD plots there is not a major conversion in CCD structure.

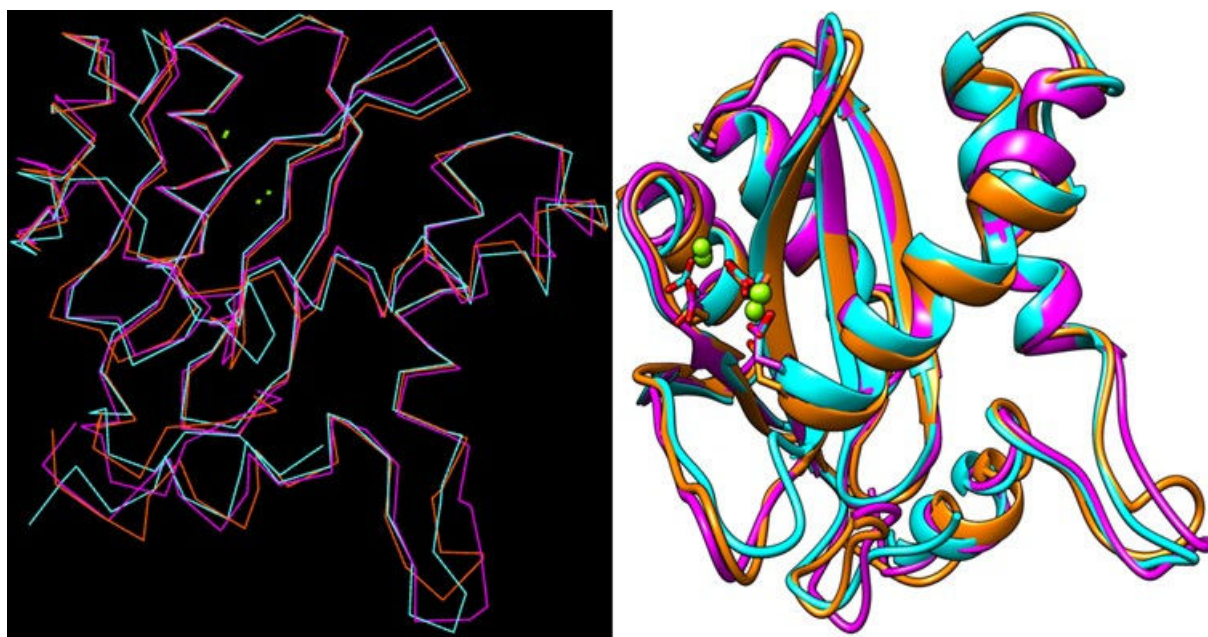


Figure 4. Superimposition of three different conformations of protein obtained from clustering analyses which are represented as C1, C2, and C3 as basic (left) and as ribbon (right) view.

Docking Studies of Ligands

The approved HIV-1 integrase inhibitors RAL, EVG, and DTG and newly designed ligands L01 (3,3'-azanediybis(2-((6,8-diaminonaphthalen-2-yl)amino)-3-oxopropanoic acid)), L02 (3,3'-azanediybis(2-((2,4-diaminopteridin-6-yl)amino)-3-oxopropanoic acid)), L03 (3,3'-azanediybis(2-((6,8-diamino-7-(3-(2-chlorophenyl)propyl)naphthalen-2-yl)amino)-3-oxopropanoic acid)) and L04 ((E)-2-((6,8-diamino-7-(3-(2-chlorophenyl)-3-oxoprop-1-en-1-yl)naphthalen-2-yl)amino)-3-oxo-3-(2-phenylacetamido)propanoic acid) were docked to CCD active site. The docking scores of ligands in C1, C2 and C3 structures are listed in Table 1 while hydrogen bonds seen between ligands and receptors and ligand atoms interacted with metals are shown in Table 2. As an example of docking, the sites of three conformations of protein which L04 posed are depicted in Figure 5 and others were shown in Supporting Information (see Figure 3). Differentiation of docking ligand to three conformations of protein structure obviously seen from figure. L04 is the best scored ligand

in C1 while L01 has best score in both C1 and C3. All ligands seem to be best docked to C1 conformation of protein except EVG. Its docking score higher in C3 than in C1.

Table 1. Docking scores (kcal/mole) of ligands in different conformations of catalytic core domain.

	C1	C2	C3
L01	-11.55	-11.08	-11.50
L02	-9.06	-8.04	-7.44
L03	-11.31	-10.09	-9.87
L04	-12.14	-9.28	-8.34
DTG	-11.70	-10.69	-11.21
EVG	-10.90	-10.32	-11.04
RAL	-11.49	-9.98	-9.31

Unsurprisingly, the docking scores of ligands, their docked place in catalytic center and the interactions of ligands with receptor are different from each other. These results were expected to some degree, on the other hand the confirmation given by the calculation presented in this study is also is an important element in the field of drug discovery. The docking score of L04 is -12.14 kcal/mole in C1 conformation of receptor while -8.34 kcal/mole in C3 conformation of receptor. We can think like this: Anyone who searches for a ligand library may eliminate L04 in C3 conformation of receptor due to its low docking score. And also this result directs us to MD simulations. Because we use MD simulations to detail dynamics and behaviors of protein or complexes. So the MD simulation analyses of complexes will inform us to know if a ligand having different orientation, docking score and interactions in different conformation of a receptor will change to same orientation and give same interactions with protein after MD simulation or not.

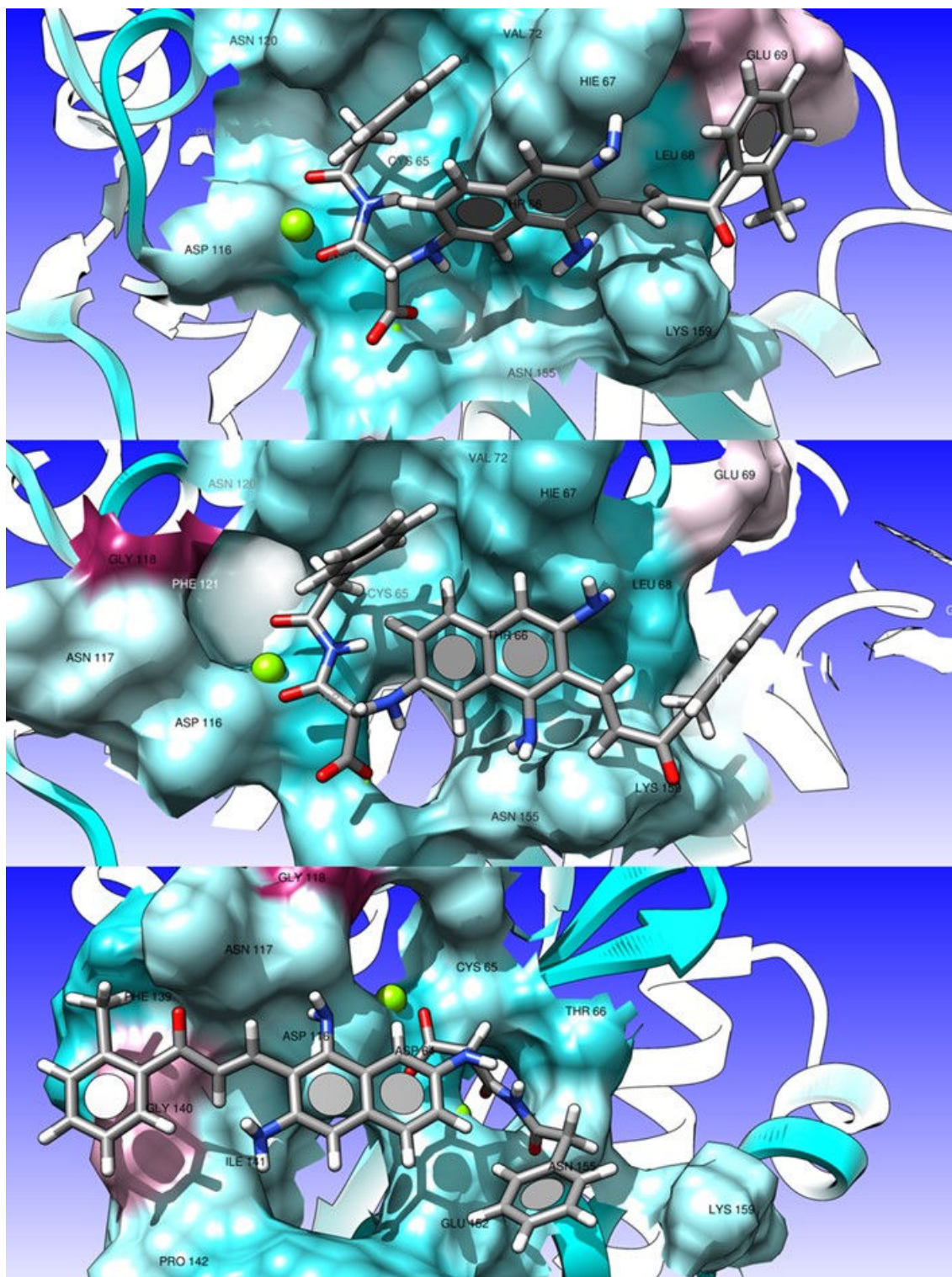


Figure 5. Docking sites and orientations of L04 in C1, C2, and C3 protein conformations.

RAL, EVG, and DTG have been used in many theoretical and experimental studies [40, 48-50]. Recently, crystal structures of PFV integrase with viral DNA including RAL, EVG, and DTG have been obtained. From these structures, 3L2V.pdb and 3OYA.pdb contain RAL, 3L2U.pdb contains EVG and 3S3M.pdb contains DTG. While Raltegravir interacts with

Tyr212 and Gly215 equivalent residues of HIV-1 IN Tyr143 and Gln146, it is also in interaction with Pro214 (Pro145 in HIV-1 IN) in 3OYA crystal structure. In their contained structures, EVG and DTG interact with same residues and also DTG interact with Glu221 (Glu152 in HIV1) in addition to Tyr212 and Pro214 residues. Notwithstanding our docking studies show that in all three conformation of protein, RAL interacts with Tyr143, the docked position of RAL is very different from position it is placed in crystal structure. This is referred to flexible loop, being in very different conformations in PFV structures and 1BL3 structure (used in this study), and also is referred to PFV having vDNA in catalytic site. The docking test of EVG to 3L2U crystal structure supports our consideration (Supporting information, see Figure 4). Performed test run docked the ligand pretty much to the same position of crystal structure while only some substituents of ligand are in different conformations. It is also must be noted that existence of DNA or RNA in structure changes docking results positively (EVG docking test score is 17.6 kcal/mole). Sharma *et al.* have also reported this issue in their study [19]. Besides, one must bear in mind that docking programs consider crystal structures containing ligand for developing program algorithms.

From Table 2 it has been seen that while all ligands interact with Mg atoms, some of ligands have four oxygen atoms in interaction with two Mg atoms. HIE67, GLU92, and ASN117 residues are found to create H bond with ligand atoms. The interactions of all ligands with protein residues at their docked sites are generally given in Table 3. C1 conformation of protein has vdW interactions with all ligands. It is consistent with docking scores of ligands.

Table 2. Hydrogen bonds and metal contacts obtained from docking results between ligand atoms and protein residues.

	C1		C2		C3	
	H bonds (Residue and Ligand atoms)	Mg-Ligand atoms	H bonds (Residue and Ligand atoms)	Mg-Ligand atoms	H bonds (Residue and Ligand atoms)	Mg-Ligand atoms
L01	GLU152OE1-H49 GLN148OE1-H47 ASN117OD1-H61	MG210-O18,O27 MG211-O17,O26	HIE67O-H48 HIE67ND1-H45 ASP116OD1-H53 ASN117O-H62	MG210-O23,O21 MG211-O18, O27	ASN117O-L01H62 ASN155HD22-L01O17 HIE67O-H48 ASP116OD1-L01H53	MG210-O23,O21 MG211-O18,O27
L02	HIE67H-O LYS159HZ1-N4 LYS159HZ3-N5 CYS65O-H GLU92OE1-H7 GLU92OE2-H11 THR66HA-O	MG210-O3,O5 MG211-O2	HI67HN-N10 ASN155HD22-O5 GLU92OE1-H3 GLU92OE2-H4 SER119OG-H5,H6 HIE67ND1-H9	MG210-O2 MG211-O4	LYS159HZ1-L02N11 ASP116OD2- L02H2 ASN117O- L02H3 GLU152OE1- L02H7 LYS156HE2- L02N11	MG210-O2 MG211-O4,O3
L03	HIE67ND1-H7 ASN155HD21-O5 ASN155HD22-O5 LYS156HZ2-O4 LYS156HZ3-O4 LYS156HZ3-O5	MG210-O,O2 MG211-O,O1,O4	ASP116OD1-H1 CYS65O-H6 HIE67ND1-H10	MG210-O, O1 MG11-O2,O5	HIE67O-L03H3 ASP116OD2-L03H3 ASP116OD2-L03H10 ASN117O-L03H9	MG210-O4 MG211-O2
L04	LYS159HZ2-O4 LYS159HZ3-N2 THR66OG1-H HIE67O-H2 HIE67ND1-H5	MG210-O,O1 MG211-O3	LYS159HZ1-O4 ASP64OD2-H CYS65O-H1 HIE67O-H5,	MG210-O,O1; MG211-O3	ASN117HD22-L04O4 ASN155HD22-L04O ASP116OD2-L04H3 ASN117O-H	MG210-O2 MG211-O1,O3,O

Table 3. Hydrogen bonds and metal contacts obtained from docking results between ligand atoms and protein residues (Continued).

	C1		C2		C3	
	H bonds (Residue and Ligand atoms)	Mg-Ligand atoms	H bonds (Residue and Ligand atoms)	Mg-Ligand atoms	H bonds (Residue and Ligand atoms)	Mg-Ligand atoms
DTG	GLU152OE1-H13 LYS156HZ1-F LYS156HZ3-F1	MG210-O2,O3 MG211-O2,O4	GLU92OE1-H3 CYS65O-H8 GLU152OE1-H4	MG210-O3,O2,O1 MG211-O2,O4	HIE67H-DTGO ASN155HD22-DTGO1 SER119H-DTGF1 SER119H-F30 HIE67O-DTGH6,H7 GLU92OE1-DTGH13,H14 GLU92OE2-DTGH9	MG210-O4,O2 MG211-O3,O2,O1
EVG	THR66OG1-H21 HIE67-H8 GLU152OE1-H20	MG210-O,O4 MG211-O2,O3	ASN117O-H21 ASP64OD1-H20 ASN117O-H10,	MG210-O2 MG211-O,O4	CYS65O-EVGH21 GLU92OE2-EVGH21 THR66HA-EVGO3 CYS65O-EVGH ASN117O-EVGH10	MG210-O2 MG211-O4,O
RAL	CYS65H-O2 GLU152OE2-H13 GLY118HA3-N4 TYR143HA-F CYS65O-H2	MG210-O2,O4 MG211-O1	LYS159HZ2-RALN4 GLU152OE1-RALH15	MG210-O,O1 MG211-O4,O1	HIE67H-RALO2 THR66HA-RALO2 HIE67HD2-RALN4 GLU92OE2-RALH1 GLU92OE1-RALH15	MG210-O,O1 MG211-O4,O1

Table 4. Various interactions between ligand atoms and protein residues composed by docking.

	C1	C2	C3
L01	n-cation: LYS156NZ vdW: ASP64, CYS65, THR66, GLY140, ILE141, ASN155, LYS159	n-sigma: HIE67 vdW: ASP64, THR66, LEU68, GLY118, ASN155, LYS159	vdW: CYS65, THR66, GLY118
L02	ASP64, THR66, ASP116, GLU152	vdW: THR66, ASN117, GLY118, GLU152	n-alkyl: LYS156 vdW: CYS65, THR66, GLY118, ASN155, LYS156
L03	Charge interactions: LYS156, THR66, VAL72, TYR143, GLU92 vdW: ASP64, CYS65, ASP116, ILE141, PRO142, GLN148, LYS159	n-sigma:THR66 Charge interactions: HIE67 vdW: LEU68, GLU92, ASN117, GLY118, SER119, ASN120, LYS159	n-p: TYR143 n-cation: LYS159 Charge interactions: LEU68, LYS159 vdW: ASP64, THR66, GLY118, TYR143, GLU152, ASN155, ILE162,
L04	Charge interactions: LEU68, HIE67 vdW: ASP64, CYS65, GLU69, GLY70, VAL72, GLU92, ASP116, GLU152, ASN155	n-sigma:THR66 Charge interactions: LEU68, LYS159 VAL72, ASP116	Charge interactions: PHE139 vdW: ASP64, CYS65, GLY140, PRO142, TYR143, GLU152
DTG	Charge interactions: HIE67, VAL72, LYS156 vdW: ASP64, CYS65, THR66, GLU92, ASP116, GLN148, ASN155	Charge interactions: HIE67, VAL72 vdW: ASP64, THR66, ASP116, TYR143, ASN155, LYS159	Charge interactions: CYS65 n-lone pair vdW: ASP64, THR66, ASP116, ASN117, GLY118, GLU152
EVG	n-sigma: THR66 vdW: CYS65, HIE67, VAL72, GLU92, ASP116, GLN148, GLU152, ASN155, LYS156, LYS159	vdW: CYS65, GLU92, GLY118, PRO142, TYR143, GLU152	vdW: THR66, HIE67, GLY118, GLY140, ILE141, PRO142, TYR143, GLU152, ASN155
RAL	Charge interactions: ILE141 vdW: THR66, HIE67, ASN117, SER119, TYR143, ASN144, ASN155	n-p T-shaped:TYR143 Charge interactions: LEU68 vdW: ASP64, CYS65, THR66, GLU92, ASP116, ASN155	n-p t-shaped: HIE67 Charge interactions: HIE67, VAL72 vdW: CYS65, ALA91, ASN117 GLY118, THR143, ASN155

Molecular Dynamics Studies of the Complexes

From the RMSD plots of complexes versus time, it is seen that the proteins reached stable states (Figure 6). In the plot of C1 complex of Dolutegravir, an ascension is seen at about 1.5-5 ns. MD movies of this complex showed the flexible loop between residues 185-198 are causing this rise. It is also seen from the RMSD plots of mentioned residues (not shown here).

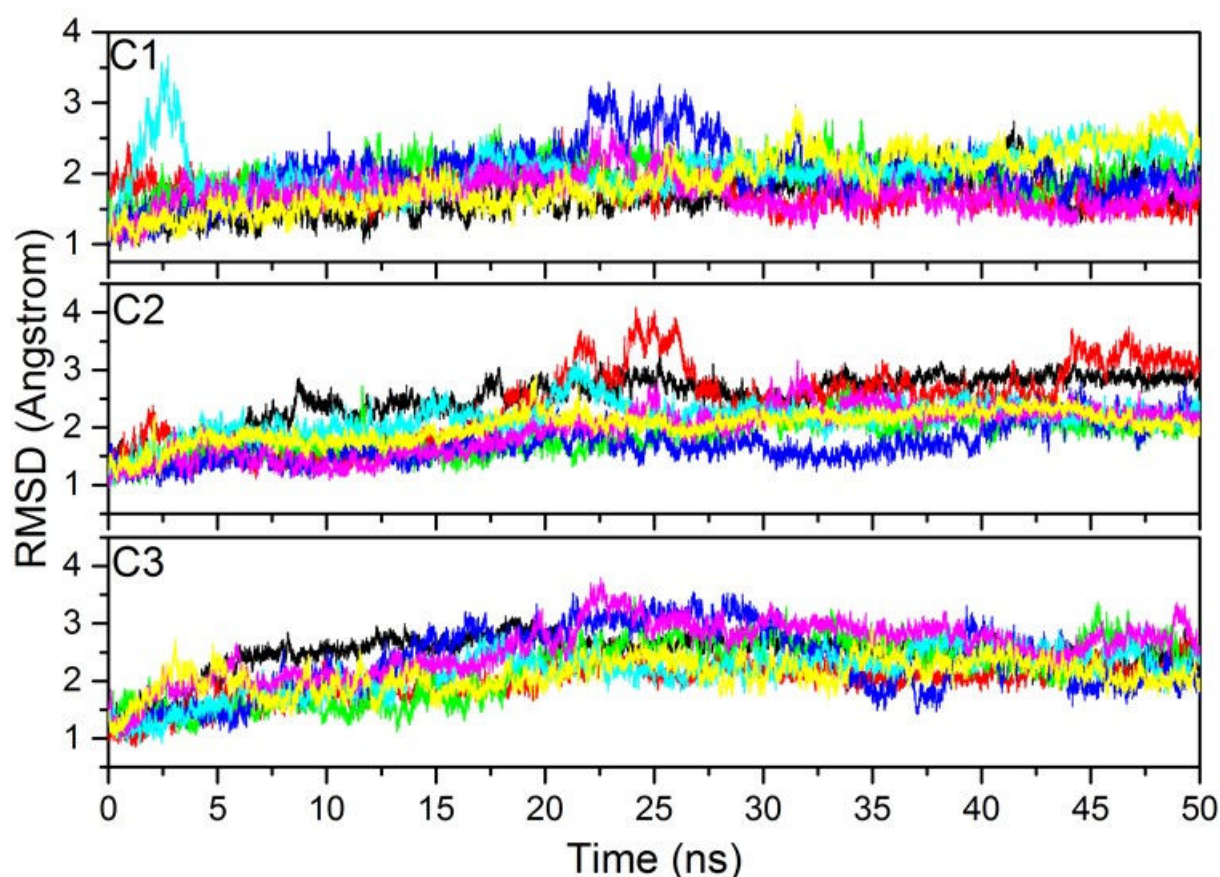


Figure 6. The time evolution of RMSD values for backbone atoms of complexes, C1, C2, and C3 (L01 black, L02 red, L03 green, L04 blue, DTG cyan, EVG magenta, and RAL yellow).

All ligands seem to be in a stable state despite the high RMSD values of L02 and L03 in C1 (Figure 7). We also determined the ligands docked to different conformations of protein with diverse orientations and interactions did not resemble each other by MD simulations (Figure 8). As an example, L01 docked to three different conformations of protein. Each docking orientation is different. And it could be seen that MD simulation did not put those three orientations of L01 to the same position (Figure 8). We would like to point out that this is not an absolute result because an MD simulation of 50 ns (a sufficient time for an MD simulation) was performed in this study and it is not definite to know there will be a change or not by extending time. However, the clustering analyses performed for the 50 ns simulation show that the conformations of complexes are close to each other and so it

is not necessary to depict the achieved clusters here. By the way, the images of structures having lowest energies illustrated here for each complex.

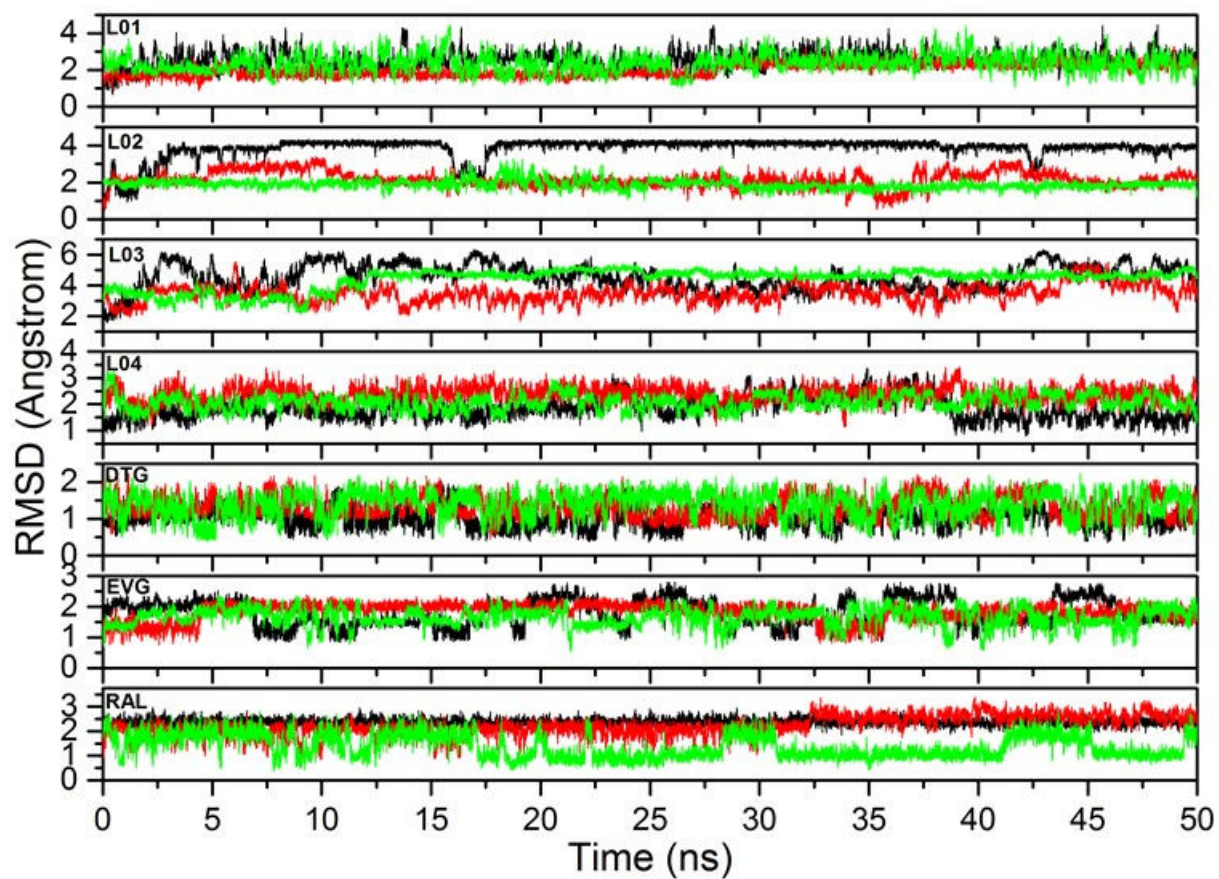


Figure 7. 50 ns time evolution of RMSD values of ligand atoms (C1 black, C2 red, and C3 green).

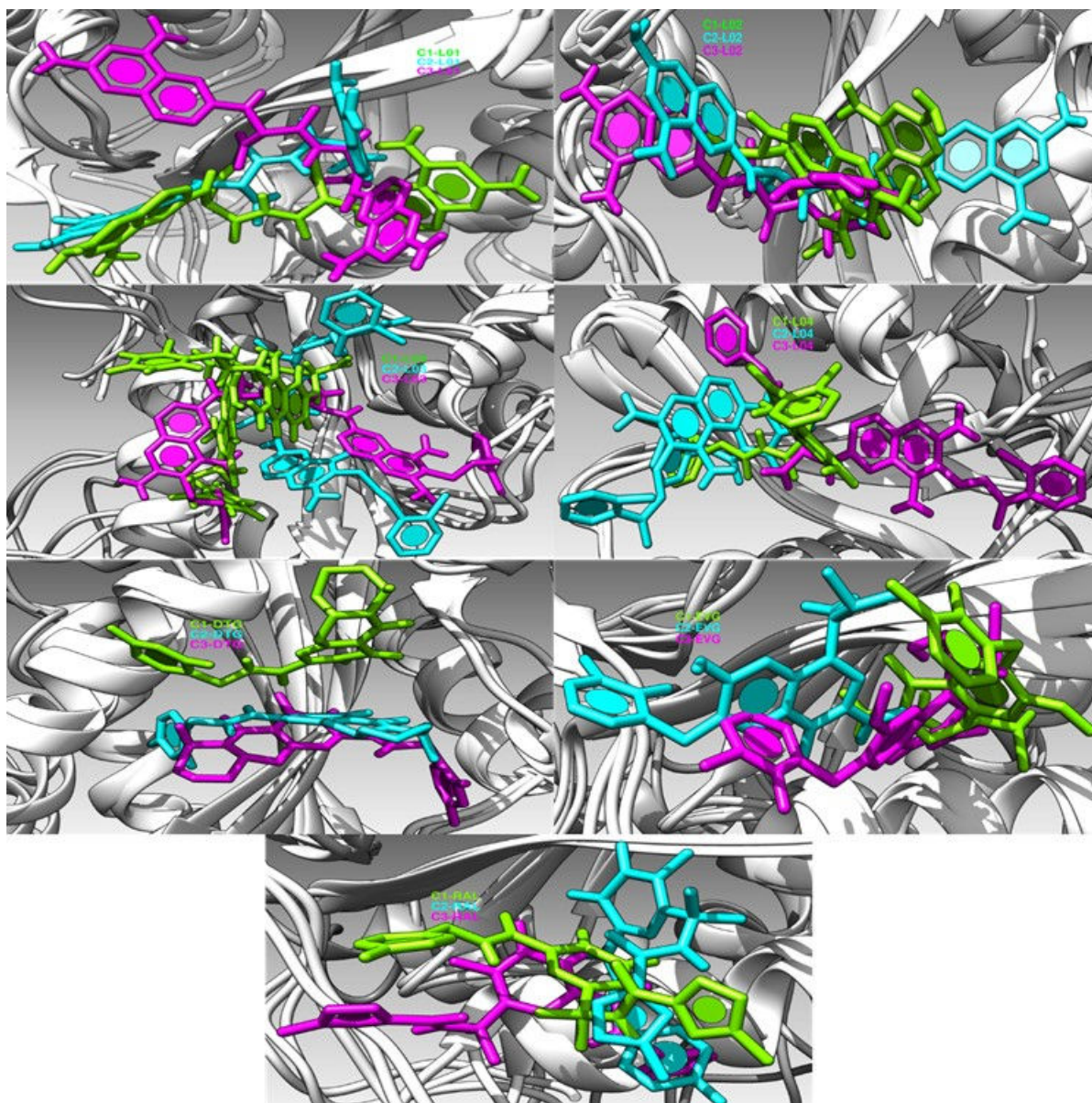


Figure 8. The positions of ligands in each protein structure. Superimposed structures are taken from a lower-energy structure of each complex's MD simulation.

Ligand-residue interactions, which are observed from docking results, seem to change significantly by MD simulations. Especially, most of hydrogen bonds and electrostatic interactions of ligands with residues obtained from docking disappeared by MD simulations (Table 4).

Table 5. Ligand-residue interactions observed from the structures with lowest energies located from MD simulations.

	C1	C2	C3
L01	vdW: ASP64, HIE67, ASP116, 3 water molecules H bonds: 1 water molecule	n-n T shaped: HIE67 vdW: CYS65, HIE67, ASN117, PHE139, LYS159 and 3 water molecules H bonds: THR66, ASP116, ASN155 and 1 water molecule	vdW: ASP64, CYS65, GLU92, ASP116, GLY118, ASN120, GLU152 and 1 water molecule H bonds: THR66, SER119, ASN155 and 4 water molecules
L02	THR66, CYS65, ASP116, ASN155, 2 water molecules H bonds: GLU152 and 4 water molecules	n-alkyl: LYS156, LYS159 vdW: TCYS65, HIE67, ASN117, GLU152, ASN155 and 1 water molecule H bonds: THR66, LYS159 and 1 water molecule	Electrostatic: LYS159 vdW: ASP64, CYS65, ASP116, GLY118, GLU152 and 2 water molecules H bonds: SER119, ASN120, ASN155 and 3 water molecules
L03	vdW: THR66, HIE67, LEU68, ASP116, ASN117, ASN155 and 2 water molecules H bonds: 1 water molecule	n-n stacked: HIE67 n-alkyl: HIE67 vdW: CYS65, THR66, GLY70, GLU92, ASN117 and 2 water molecules H bonds: ASP64, ASP116, GLU152, ASN155 and 2 water molecules	Electrostatic: ASP64 Amid n-stacked: ALA91 n-alkyl: VAL72, LYS159 alkyl-alkyl: LEU68 vdW: THR66, HIE67, ILE89, PRO90, GLU92, SER119, ASN120, ASN155, LEU158, ILE162 and 3 water molecules H bonds: CYS65, ASP116 and 1 water molecule
L04	vdW: ASP64, THR66, GLU69, HIE67, VAL72, ILE73, ASP116, GLU152 and 4 water molecules n-alkyl: CYS65	n-n T shaped: HIE67 vdW: ASP64, CYS65, THR66, GLU92, ASP116 and 4 water molecules	n-cation: LYS159 n-alkyl: TYR143, PRO145 vdW: ASP64, THR66, HIE67, ASP116, GLU152, ASN155 and 2 water molecules H bonds: 1 water molecule
DTG	vdW: ASP64, ASP116, ILE141, TYR143 H bonds: GLN148 and 2 water molecules	n-alkyl: LYS159 vdW: CYS65, THR66, ASP116, GLU152, ASN155, LYS156 and 1 water molecule H bonds: 1 water molecule	vdW: CYS65, GLU92, ASP92, ASP116, GLY118, GLU152, LYS159 and 3 water molecules H bonds: ASN155 and 1 water molecule
EVG	vdW: ASP64, THR66, HIE67, ASP116, ASN155, LYS159 and 5 water molecules H bonds: GLN148 and 2 water molecules	n-anion: ASP116 vdW: ASP64, GLY118, PHE139, GLY140, GLU152 and 4 water molecules H bonds: ASN117 and 2 water molecules	n-anion: ASP64 vdW: HIE67, GLU92, ASP116, GLU152 and 2 water molecules H bonds: CYS65, THR66, ASN155 and 1 water molecule
RAL	n-n stacked: TYR143 vdW: ASP64, ASP116 and 2 water molecules H bonds: 1 water molecule	vdW: ASP64, CYS65, THR66, HIE67, ASP116, TYR143, LYS159 and 5 water molecules H bonds: 1 water molecule	alkyl-alkyl: ILE141 n-anion: GLU152 vdW: ASP64, ASP116, TYR143, LYS156, LYS159 and 4 water molecules

Binding Free Energies of Ligands

The binding modes of the ligands to the different conformations of HIV-1 integrase catalytic core domain were competed by end point energy method, (MM-PB(GB)/SA). Calculated values are shown in Table 5.

Table 6. Binding free energies of ligands calculated by MM-PB(GB)SA method and contribution of entropy to binding free energies.

	ΔE_{elec}	ΔE_{vdW}	ΔG_{PB}	ΔG_{GB}	-TAS	ΔG_{bind}^{PB}	ΔG_{bind}^{GB}
C1_L01	-482.0850	-4.2186	-13.0748	-16.5701	28.6627	15.5879	12.0926
C1_L02	-413.9868	-3.1813	-2.3425	-5.6870	22.4444	20.1019	16.7574
C1_L03	-512.5300	-13.5305	-35.9332	-49.3102	27.2606	-8.6726	-22.0496
C1_L04	-294.7430	-9.4281	-14.7613	-2.3909	24.3747	9.6134	21.9838
C1_DTG	-336.6129	-8.0492	-7.5524	-11.5279	23.6320	16.0796	12.1041
C1_EVG	-422.7991	-1.9412	-39.7112	-41.0937	24.8457	-14.8655	-16.2480
C1_RAL	-278.8543	-6.2337	0.0161	-2.4443	21.3160	21.3321	18.8717
C2_L01	-539.7636	-5.0295	-49.4787	-52.4085	27.7591	-21.7196	-24.6494
C2_L02	-532.3656	-6.4072	-25.1195	-15.7172	26.7391	1.6196	11.0219
C2_L03	-512.5300	-13.5305	-35.9332	-49.3102	30.7403	-5.1929	-18.5699
C2_L04	-296.6142	-6.6585	-13.3614	0.3272	22.4650	9.1036	22.7922
C2_DTG	-338.2980	-0.1855	-17.6762	-7.9015	25.0018	7.3256	17.1003
C2_EVG	-311.6691	-7.5985	-8.0243	-16.2065	24.9792	16.9549	8.7727
C2_RAL	-277.6655	-9.7355	-3.8454	-4.3016	20.6870	16.8416	16.3854
C3_L01	-518.1380	-6.6245	-4.8480	-34.2500	29.0603	24.2123	-5.1897
C3_L02	-443.3987	-13.3996	6.4690	-11.4051	28.1492	34.6182	16.7441
C3_L03	-498.7371	-27.6130	-31.0748	-37.0633	31.3367	0.2619	-5.7266
C3_L04	-279.6095	-14.7686	3.2340	-9.2501	26.8973	30.1313	17.6472
C3_DTG	-338.2980	-0.1855	-17.6762	-7.9015	25.8882	8.2120	17.9867
C3_EVG	-383.1383	-3.2655	-37.1270	-35.7265	25.2536	-11.8734	-10.4729
C3_RAL	-285.5304	-10.2197	-9.3601	-3.8106	-22.5998	13.2397	18.7892

ΔE_{elec} : Contribution of electrostatic energy to binding energy, ΔE_{vdW} : Contribution of van der Waals interactions to binding energy, ΔG_{PB} and ΔG_{GB} : Binding energies according to Poisson-Boltzmann and Generalized-Born methods. Mean energies are in kcal mol⁻¹.

Binding free energies of ligands were calculated by Poisson-Boltzmann (PB) [37, 51] and Generalized-Born (GB) [37, 51] approaches. As the varying docking scores, interactions and orientations of ligands in different conformations of protein, binding free energies of ligands also differ from each other. In general, the scores of PB approach are at the lowest than scores of GB approach but in this study some of ligands gave greater PB scores than GB scores such as c1_L04, c2_L02, c2_L04, c2_dtg and c3_dtg/evg/ral. In the complexes which ligands having low binding energy, the electrostatic contributions seem to be lower and mainly the lower binding energy values are complying with this parameter.

From all ligands, the best binding free energy belongs to L01 in C2 protein while Elvitegravir shows favorable values except in C2 protein ($C1_{PB}$: -39.71, $C1_{GB}$: -41.09, $C3_{PB}$: -37.13, $C3_{GB}$: -35.73). Elvitegravir is also well bounded to protein than RAL and DTG inhibitors. The most surprising result is that Raltegravir seems to be the worst ligand overall ligands according to binding free energies. Besides, it has the lowest average binding score in three conformations of protein. This situation is also in contrast with conception of RAL binds rather electrostatically to protein because obtained electrostatic energies of RAL are low in generally.

From the designed ligands, while the results of L01 and L03 are favorable, L04, which has the best docking score (-12.09 kcal/mole) in C3 complex showed low binding free energies (ΔG_{PB} : 3.23 and ΔG_{GB} : -9.25) in contrast to its docking score. Nevertheless, from plotting (Figure 9) docking scores with binding free energies of ligands, it has seen in general the docking scores of ligands are compatible with their binding free energies. We can make an inference that used docking program has a strong estimating property of binding free energies.

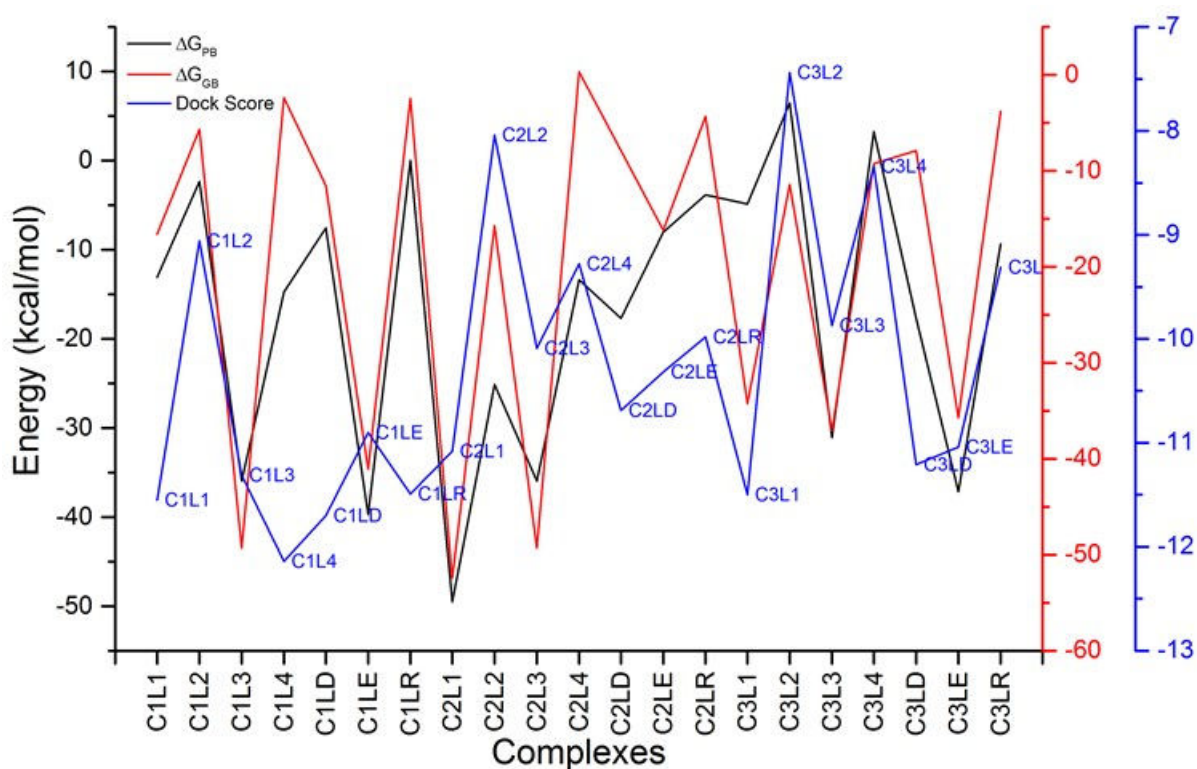


Figure 9. The relation between docking scores and binding free energies calculated by MM-PB(GB)SA.

The contribution of entropy to binding free energies were also computed. While electrostatic energies, vdW energies, and non-polar solvation terms have positive

contribution on binding ligands to protein, polar solvation and entropy terms have negative effect on binding ligands.

CONCLUSION

As a conclusion, three ligands which are currently in use as HIV-1 Inhibitors and four newly designed ligands were used in this study. A molecular dynamics simulation of 10 ns was performed to protein before docking studies. And docking studies were run for three conformations of protein obtained from cluster analyses. Ligands are bound to three conformations of protein in different orientations and so have diverse binding free energies. L04 is the ligand having best docking score (-12.14 kcal/mole) in C1 protein conformation while docking of L02 into C3 protein conformation has the lowest docking score (-7.44 kcal/mole).

After docking studies, a 50 ns MD simulation was performed for each complex and results were analyzed. Ligands' binding free energy calculations were carried out by MM-PB(GB)SA and the results were contributed by entropy calculations. The calculations showed that the binding of L01 to C2 protein is the best bound ligand over other ligands. Besides, ligand having the best docking score, L04, did not demonstrate a good binding to protein. This issue was the one of purposes to search in study and we can say that docking scores could believe a researcher for selecting proper ligands, according to results. It is also should be noted the MM-PB(GB)SA calculations could not produce absolute experimental results but produce outcomes those are compatible with experimental results [52-54].

Another aim of the study was to evaluate new molecules as new HIV-IN inhibitors. From designed ligands L01 (3,3'-azanediybis(2-((6,8-diaminonaphthalen-2-yl)amino)-3-oxopropanoic acid)) and L03 (3,3'-azanediybis(2-((6,8-diamino-7-(3-(2-chlorophenyl)propyl)naphthalen-2-yl)amino)-3-oxopropanoic acid)) showed promising results. As the last aim of this study, we could see that MD calculations do not convert conformations of different oriented ligands (in different conformations of protein) to same positions in terms of location and interactions of ligand protein. We also should remark that even though the simulations were carried out for a meaningful time of MD calculations, it is only a simulation of 50 ns and so those issues may vary *in vivo*.

ACKNOWLEDGMENTS

The author is grateful to the Research Foundation of Batman University (Project 2012-FED-7) for the financial support.

REFERENCES

1. Global Aids Response Progress Reporting 2015. 2015. www.unaids.org/sites/default/files/media.../JC2702_GARPR2015guidelines_en.pdf.
2. Miri L, Bouvier G, Kettani A, Mikou A, Wakrim L, Nilges M, Malliavin TE. Stabilization of the integrase-DNA complex by Mg²⁺ ions and prediction of key residues for binding HIV-1 integrase inhibitors. *Proteins*. 2014;82(3):466-78.10.1002/prot.24412.
3. Pendri A, Meanwell NA, Peese KM, Walker MA. New first and second generation inhibitors of human immunodeficiency virus-1 integrase. *Expert Opin Ther Patents*. 2011;21(8):1173-89.10.1517/13543776.2011.586631.
4. Zhang D, Debnath B, Yu S, Sanchez TW, Christ F, Liu Y, Debyser Z, Neamati N, Zhao G. Design and discovery of 5-hydroxy-6-oxo-1,6-dihydropyrimidine-4-carboxamide inhibitors of HIV-1 integrase. *Bioorganic & medicinal chemistry*. 2014;22(19):5446-53.10.1016/j.bmc.2014.07.036.
5. Mehellou Y, De Clercq E. Twenty-six years of anti-HIV drug discovery: where do we stand and where do we go? *J Med Chem*. 2010;53(2):521-38.10.1021/jm900492g.
6. De Luca L, De Grazia S, Ferro S, Gitto R, Christ F, Debyser Z, Chimirri A. HIV-1 integrase strand-transfer inhibitors: design, synthesis and molecular modeling investigation. *Eur J Med Chem*. 2011;46(2):756-64.10.1016/j.ejmech.2010.12.012.
7. DeGruttola V, Dix L, D'Aquila R, Holder D, Phillips A, Ait-Khaled M, Baxter J, Clevenbergh P, Hammer S, Harrigan R, Katzenstein D, Lanier R, Miller M, Para M, Yerly S, Zolopa A, Murray J, Patick A, Miller V, Castillo S, Pedneault L, Mellors J. The relation between baseline HIV drug resistance and response to antiretroviral therapy: re-analysis of retrospective and prospective studies using a standardized data analysis plan. *Antiviral therapy*. 2000;5(1):41-8,1359-6535 (Print)
8. Goethals O, Van Ginderen M, Vos A, Cummings MD, Van Der Borght K, Van Wesenbeeck L, Feyaerts M, Verheyen A, Smits V, Van Loock M, Hertogs K, Schols D, Clayton RF. Resistance to raltegravir highlights integrase mutations at codon 148 in conferring cross-resistance to a second-generation HIV-1 integrase inhibitor. *Antiviral Res*. 2011;91(2):167-76.10.1016/j.antiviral.2011.05.011.
9. Richman DD. Antiviral drug resistance. *Antiviral Res*. 2006;71(2-3):117-21.10.1016/j.antiviral.2006.03.004.
10. Calmy A, Hirschel B, Cooper DA, Carr A. A new era of antiretroviral drug toxicity. *Antiviral therapy*. 2009;14(2):165-79,1359-6535 (Print).
11. Clavel F, Hance AJ. HIV drug resistance. *N Engl J Med*. 2004;350(10):1023-35.10.1056/NEJMra025195.
12. Emini EA, Graham DJ, Gotlib L, Condra JH, Byrnes VW, Schleif WA. HIV and multidrug resistance. *Nature*. 1993;364(6439):679.10.1038/364679b0.
13. Geeraert L, Kraus G, Pomerantz RJ. Hide-and-seek: the challenge of viral persistence in HIV-1 infection. *Annu Rev Med*. 2008;59:487-501.10.1146/annurev.med.59.062806.123001.
14. Johnson VA, Brun-Vezinet F, Clotet B, Gunthard HF, Kuritzkes DR, Pillay D, Schapiro JM, Richman DD. Update of the drug resistance mutations in HIV-1: December 2010. *Top HIV Med*. 2010;18(5):156-63,2161-5845 (Electronic), 1542-8826 (Linking).
15. Malta M, Magnanini MM, Strathdee SA, Bastos FI. Adherence to antiretroviral therapy among HIV-infected drug users: a meta-analysis. *AIDS Behav*. 2010;14(4):731-47.10.1007/s10461-008-9489-7.

16. Marcello A. Latency: the hidden HIV-1 challenge. *Retrovirology*. 2006;3:7.10.1186/1742-4690-3-7.
17. Moyle G, Gatell J, Perno CF, Ratanasuwan W, Schechter M, Tsoukas C. Potential for new antiretrovirals to address unmet needs in the management of HIV-1 infection. *AIDS Patient Care STDS*. 2008;22(6):459-71.10.1089/apc.2007.0136.
18. Paredes R, Clotet B. Clinical management of HIV-1 resistance. *Antiviral Res*. 2010;85(1):245-65.10.1016/j.antiviral.2009.09.015.
19. Sharma H, Sanchez TW, Neamati N, Detorio M, Schinazi RF, Cheng X, Buolamwini JK. Synthesis, docking, and biological studies of phenanthrene beta-diketo acids as novel HIV-1 integrase inhibitors. *Bioorg Med Chem Lett*. 2013;23(22):6146-51.10.1016/j.bmcl.2013.09.009.
20. Ercan S, Pirinccioglu N. Computational design of a full-length model of HIV-1 integrase: modeling of new inhibitors and comparison of their calculated binding energies with those previously studied. *J Mol Model*. 2013;19(10):4349-68.10.1007/s00894-013-1943-4.
21. Desimmie BA, Demeulemeester J, Suchaud V, Taltynov O, Billamboz M, Lion C, Bailly F, Strelkov SV, Debyser Z, Cotelle P, Christ F. 2-Hydroxyisoquinoline-1,3(2H,4H)-diones (HIDs), novel inhibitors of HIV integrase with a high barrier to resistance. *ACS Chem Biol*. 2013;8(6):1187-94.10.1021/cb4000426.
22. Summa V, Petrocchi A, Bonelli F, Crescenzi B, Donghi M, Ferrara M, Fiore F, Gardelli C, Gonzalez Paz O, Hazuda DJ, Jones P, Kinzel O, Laufer R, Monteagudo E, Muraglia E, Nizi E, Orvieto F, Pace P, Pescatore G, Scarpelli R, Stillmock K, Witmer MV, Rowley M. Discovery of raltegravir, a potent, selective orally bioavailable HIV-integrase inhibitor for the treatment of HIV-AIDS infection. *J Med Chem*. 2008;51(18):5843-55.10.1021/jm800245z.
23. Sax PE, DeJesus E, Mills A, Zolopa A, Cohen C, Wohl D, Gallant JE, Liu HC, Zhong L, Yale K, White K, Kearney BP, Szwarcberg J, Quirk E, Cheng AK, team G-U-s. Co-formulated elvitegravir, cobicistat, emtricitabine, and tenofovir versus co-formulated efavirenz, emtricitabine, and tenofovir for initial treatment of HIV-1 infection: a randomised, double-blind, phase 3 trial, analysis of results after 48 weeks. *Lancet*. 2012;379(9835):2439-48.10.1016/S0140-6736(12)60917-9.
24. Dow DE, Bartlett JA. Dolutegravir, the Second-Generation of Integrase Strand Transfer Inhibitors (INSTIs) for the Treatment of HIV. *Infect Dis Ther*. 2014;3(2):83-102.10.1007/s40121-014-0029-7.
25. Delelis O, Carayon K, Saib A, Deprez E, Mouscadet JF. Integrase and integration: biochemical activities of HIV-1 integrase. *Retrovirology*. 2008;5:114.10.1186/1742-4690-5-114.
26. Wang JY, Ling H, Yang W, Craigie R. Structure of a two-domain fragment of HIV-1 integrase: implications for domain organization in the intact protein. *EMBO J*. 2001;20(24):7333-43.10.1093/emboj/20.24.7333.
27. Chen JC, Krucinski J, Miercke LJ, Finer-Moore JS, Tang AH, Leavitt AD, Stroud RM. Crystal structure of the HIV-1 integrase catalytic core and C-terminal domains: a model for viral DNA binding. *Proc Natl Acad Sci U S A*. 2000;97(15):8233-8.10.1073/pnas.150220297.
28. Maignan S, Guilloteau JP, Zhou-Liu Q, Clement-Mella C, Mikol V. Crystal structures of the catalytic domain of HIV-1 integrase free and complexed with its metal cofactor: high level of similarity of the active site with other viral integrases. *Journal of molecular biology*. 1998;282(2):359-68.10.1006/jmbi.1998.2002.
29. Bujacz G, Alexandratos J, Qing ZL, Clement-Mella C, Wlodawer A. The catalytic domain of human immunodeficiency virus integrase: ordered active site in the F185H mutant. *FEBS letters*. 1996;398(2-3):175-8,0014-5793 (Print).
30. Goldgur Y, Craigie R, Cohen GH, Fujiwara T, Yoshinaga T, Fujishita T, Sugimoto H, Endo T, Murai H, Davies DR. Structure of the HIV-1 integrase catalytic domain complexed with an inhibitor: a platform for antiviral drug design. *Proc Natl Acad Sci U S A*. 1999;96(23):13040-3,0027-8424 (Print).

31. Wang Y, Rong J, Zhang B, Hu L, Wang X, Zeng C. Design and synthesis of N-methylpyrimidone derivatives as HIV-1 integrase inhibitors. *Bioorganic & medicinal chemistry*. 2015;23(4):735-41.10.1016/j.bmc.2014.12.059.
32. Costi R, Metifiot M, Chung S, Cuzzucoli Crucitti G, Maddali K, Pescatori L, Messori A, Madia VN, Pupo G, Scipione L, Tortorella S, Di Leva FS, Cosconati S, Marinelli L, Novellino E, Le Grice SF, Corona A, Pommier Y, Marchand C, Di Santo R. Basic quinolinonyl diketo acid derivatives as inhibitors of HIV integrase and their activity against RNase H function of reverse transcriptase. *J Med Chem*. 2014;57(8):3223-34.10.1021/jm5001503.
33. Hare S, Gupta SS, Valkov E, Engelman A, Cherepanov P. Retroviral intasome assembly and inhibition of DNA strand transfer. *Nature*. 2010;464(7286):232-6.10.1038/nature08784.
34. Chen Q, Cheng X, Wei D, Xu Q. Molecular dynamics simulation studies of the wild type and E92Q/N155H mutant of Elvitegravir-resistance HIV-1 integrase. *Interdiscip Sci*. 2015;7(1):36-42.10.1007/s12539-014-0235-8.
35. Brigo A, Lee KW, Iurcu Mustata G, Briggs JM. Comparison of multiple molecular dynamics trajectories calculated for the drug-resistant HIV-1 integrase T66I/M154I catalytic domain. *Biophys J*. 2005;88(5):3072-82.10.1529/biophysj.104.050286.
36. Brigo A, Lee KW, Fogolari F, Mustata GI, Briggs JM. Comparative molecular dynamics simulations of HIV-1 integrase and the T66I/M154I mutant: binding modes and drug resistance to a diketo acid inhibitor. *Proteins*. 2005;59(4):723-41.10.1002/prot.20447.
37. Miller BR, 3rd, McGee TD, Jr., Swails JM, Homeyer N, Gohlke H, Roitberg AE. MMPBSA.py: An Efficient Program for End-State Free Energy Calculations. *J Chem Theory Comput*. 2012;8(9):3314-21.10.1021/ct300418h.
38. Berman HM, Westbrook J, Feng Z, Gilliland G, Bhat TN, Weissig H, Shindyalov IN, Bourne PE. The Protein Data Bank. *Nucleic acids research*. 2000;28(1):235-42,0305-1048 (Print).
39. Sechi M, Carcelli M, Rogolino D, Neamati N. Role of Metals in HIV-1 Integrase Inhibitor Design. *HIV-1 Integrase: John Wiley & Sons, Inc.*; 2011. p. 287-307.9781118015377.
40. Metifiot M, Maddali K, Johnson BC, Hare S, Smith SJ, Zhao XZ, Marchand C, Burke TR, Jr., Hughes SH, Cherepanov P, Pommier Y. Activities, crystal structures, and molecular dynamics of dihydro-1H-isoindeole derivatives, inhibitors of HIV-1 integrase. *ACS Chem Biol*. 2013;8(1):209-17.10.1021/cb300471n.
41. DA Case TD, TE Cheatham III, CL Simmerling, J Wang, RE Duke, R Luo, RC Walker, W Zhang, KM Merz, B Roberts, S Hayik, A Roitberg, G Seabra, J Swails, AW Goetz, I Kolossváry, KF Wong, F Paesani, J Vanicek, RM Wolf, J Liu, X Wu, SR Brozell, T Steinbrecher, H Gohlke, Q Cai, X Ye, J Wang, MJ Hsieh, G Cui, DR Roe, DH Mathews, MG Seetin, R Salomon-Ferrer, C Sagui, V Babin, T Luchko, S Gusarov, A Kovalenko, PA Kollman. University of California; 2012.
42. Jorgensen WL, Chandrasekhar J, Madura JD, Impey RW, Klein ML. Comparison of simple potential functions for simulating liquid water. *The Journal of chemical physics*. 1983;79(2):926-35,0021-9606.
43. Frisch MJT, G. W.; Schlegel, H. B.; Scuseria, G. E.; Robb, M. A.; Cheeseman, J. R.; Scalmani, G.; Barone, V.; Mennucci, B.; Petersson, G. A.; Nakatsuji, H.; Caricato, M.; Li, X.; Hratchian, H. P.; Izmaylov, A. F.; Bloino, J.; Zheng, G.; Sonnenberg, J. L.; Hada, M.; Ehara, M.; Toyota, K.; Fukuda, R.; Hasegawa, J.; Ishida, M.; Nakajima, T.; Honda, Y.; Kitao, O.; Nakai, H.; Vreven, T.; Montgomery, J. A., Jr.; Peralta, J. E.; Ogliaro, F.; Bearpark, M.; Heyd, J. J.; Brothers, E.; Kudin, K. N.; Staroverov, V. N.; Kobayashi, R.; Normand, J.; Raghavachari, K.; Rendell, A.; Burant, J. C.; Iyengar, S. S.; Tomasi, J.; Cossi, M.; Rega, N.; Millam, J. M.; Klene, M.; Knox, J. E.; Cross, J. B.; Bakken, V.; Adamo, C.; Jaramillo, J.; Gomperts, R.; Stratmann, R. E.; Yazyev, O.; Austin, A. J.; Cammi, R.; Pomelli, C.; Ochterski, J. W.; Martin, R. L.; Morokuma, K.; Zakrzewski, V. G.; Voth, G. A.; Salvador, P.; Dannenberg, J. J.; Dapprich, S.; Daniels, A. D.; Farkas, Ö.; Foresman, J. B.; Ortiz, J. V.; Cioslowski, J.; Fox, D. J. *Gaussian 09, Revision E.01 ed: Gaussian, Inc., Wallingford CT*; 2009.

44. Darden T, York D, Pedersen L. Particle mesh Ewald: An $N \cdot \log(N)$ method for Ewald sums in large systems. *The Journal of chemical physics*. 1993;98(12):10089-92,0021-9606.
45. Ryckaert J-P, Ciccotti G, Berendsen HJ. Numerical integration of the cartesian equations of motion of a system with constraints: molecular dynamics of n-alkanes. *Journal of Computational Physics*. 1977;23(3):327-41,0021-9991.
46. Feig M, Karanicolas J, Brooks CL, 3rd. MMTSB Tool Set: enhanced sampling and multiscale modeling methods for applications in structural biology. *J Mol Graph Model*. 2004;22(5):377-95.10.1016/j.jmglm.2003.12.005.
47. Morris GM, Huey R, Lindstrom W, Sanner MF, Belew RK, Goodsell DS, Olson AJ. AutoDock4 and AutoDockTools4: Automated docking with selective receptor flexibility. *J Comput Chem*. 2009;30(16):2785-91.10.1002/jcc.21256.
48. Bera S, Pandey KK, Vora AC, Grandgenett DP. HIV-1 integrase strand transfer inhibitors stabilize an integrase-single blunt-ended DNA complex. *Journal of molecular biology*. 2011;410(5):831-46.10.1016/j.jmb.2011.01.043.
49. Sharma H, Cheng X, Buolamwini JK. Homology model-guided 3D-QSAR studies of HIV-1 integrase inhibitors. *J Chem Inf Model*. 2012;52(2):515-44.10.1021/ci200485a.
50. Hare S, Smith SJ, Metifiot M, Jaxa-Chamiec A, Pommier Y, Hughes SH, Cherepanov P. Structural and functional analyses of the second-generation integrase strand transfer inhibitor dolutegravir (S/GSK1349572). *Mol Pharmacol*. 2011;80(4):565-72.10.1124/mol.111.073189.
51. Homeyer N, Gohlke H. Free Energy Calculations by the Molecular Mechanics Poisson-Boltzmann Surface Area Method. *Molecular informatics*. 2012;31(2):114-22.10.1002/minf.201100135.
52. Xue W, Liu H, Yao X. Molecular mechanism of HIV-1 integrase-vDNA interactions and strand transfer inhibitor action: a molecular modeling perspective. *J Comput Chem*. 2012;33(5):527-36.10.1002/jcc.22887.
53. Kuhn B, Kollman PA. Binding of a diverse set of ligands to avidin and streptavidin: an accurate quantitative prediction of their relative affinities by a combination of molecular mechanics and continuum solvent models. *J Med Chem*. 2000;43(20):3786-91,0022-2623 (Print).
54. Wang J, Morin P, Wang W, Kollman PA. Use of MM-PBSA in Reproducing the Binding Free Energies to HIV-1 RT of TIBO Derivatives and Predicting the Binding Mode to HIV-1 RT of Efavirenz by Docking and MM-PBSA. *Journal of the American Chemical Society*. 2001;123(22):5221-30.10.1021/ja003834q.

Türkçe Öz ve Anahtar Kelimeler

Bazı Önceden Çalışılmış ve Yeni Tasarlanmış Ligandların HIV-1 İntegraz'ın Katalitik Çekirdek Bölgesine Bağlanması ve Moleküler Dinamik Hesapları ve Bağlanma Sonuçları Üzerinde Proteinin Yönelimsel Değişimlerinin Etkisinin İncelenmesi

Selami Ercan*

Öz: Günümüzde AIDS kontrolden çıkmış bir salgın hastalık görünümündedir ve HIV-1 virüsünden kaynaklanan çok sayıda ölüme neden olmaktadır. Yaklaşık 35 yıldır virus hayat çevriminin çeşitli adımlarını hedef alan ilaçlar geliştirilmiştir. HIV-1 integraz, virus hayat çevrimi için esas olan bu adımlardan birini oluşturur. Bilgisayarlı ilaç tasarımı pek çok ilacın geliştirilmesinde ve iyileştirme çalışmalarında kullanılmakta olup ilk HIV-1 integraz inhibitörü olan Raltegravir'in geliştirilmesinde de kullanılmıştır. Bu çalışmada, dört yeni tasarım ligand ile daha önce HIV-1 integraz inhibitörü olarak kullanılan üç ligandın HIV-1 integrazın katalitik merkez bölgesine bağlanması incelenmiştir. Her ligand proteinin üç farklı biçimine bağlanmıştır. Hazırlanan kompleksler (21 adet) 50 ns MD simülasyona tabi tutulmuş ve sonuçlar incelenmiştir. Son olarak, ligandların bağlanma serbest enerjileri incelenmiştir. Tasarlanan ligandlardan L01 ve L03 uygun sonuçlar vermiştir. Bir protein yapısında düşük bağlanma skoruna sahip ligandların başka bir konformasyonda daha iyi skor verip veremeyeceği ve MD simülasyonlarının, simülasyonun sonunda aynı konumda ancak farklı konumlanmış ve farklı yönlenmiş ligandları barındırıp barındırmayacağı hakkında sorulan sorulara cevap bulunmuştur.

Anahtar kelimeler: HIV-1 integraz; ilaç tasarımı; bağlanma; moleküler dinamik; bağlanma serbest enerjisi.

Sunulma: 09 Eylül 2016. **Düzenleme:** 13 Ekim 2016. **Kabul:** 24 Ekim 2016.